



# Efficient Room-Temperature Phosphorescence from Discrete Molecules Based on Thianthrene Derivatives for Oxygen Sensing and Detection

Zhiqiang Yang, Shuaiqiang Zhao, Xiangyu Zhang, Meng Liu, Haichao Liu\* and Bing Yang\*

State Key Laboratory of Supramolecular Structure and Materials, College of Chemistry, Jilin University, Changchun, China

## OPEN ACCESS

### Edited by:

Wang Zhang Yuan,  
Shanghai Jiao Tong University, China

### Reviewed by:

Zhiyong Yang,  
Sun Yat-sen University, China  
Wei Jun Jin,  
Beijing Normal University, China

### \*Correspondence:

Haichao Liu  
hcliu@jlu.edu.cn  
Bing Yang  
yangbing@jlu.edu.cn

### Specialty section:

This article was submitted to  
Physical Chemistry and Chemical  
Physics,  
a section of the journal  
Frontiers in Chemistry

Received: 06 November 2021

Accepted: 15 December 2021

Published: 27 January 2022

### Citation:

Yang Z, Zhao S, Zhang X, Liu M, Liu H  
and Yang B (2022) Efficient Room-  
Temperature Phosphorescence from  
Discrete Molecules Based on  
Thianthrene Derivatives for Oxygen  
Sensing and Detection.  
Front. Chem. 9:810304.  
doi: 10.3389/fchem.2021.810304

In this work, two thianthrene (TA) derivatives, 1-phenylthianthrene (TA1P) and 2-phenylthianthrene (TA2P), were synthesized with single-phenyl modification for pure organic discrete-molecule room-temperature phosphorescence (RTP). They both show the dual emission of fluorescence and RTP in amorphous polymer matrix after deoxygenation, as a result of a new mechanism of folding-induced spin-orbit coupling (SOC) enhancement. Compared with TA1P, TA2P exhibits a higher RTP efficiency and a larger spectral separation between fluorescence and RTP, which is ascribed to the substituent effect of TA at the 2-position. With decreasing oxygen concentration from 1.61% to 0%, the discrete-molecule TA2P shows an about 18-fold increase in RTP intensity and an almost constant fluorescence intensity, which can make TA2P as a self-reference ratiometric optical oxygen sensing probe at low oxygen concentrations. The oxygen quenching constant ( $K_{SV}$ ) of TA2P is estimated as high as  $10.22 \text{ KPa}^{-1}$  for polymethyl methacrylate (PMMA)-doped film, and even reach up to  $111.86 \text{ KPa}^{-1}$  for Zeonex<sup>®</sup>-doped film, which demonstrates a very high sensitivity in oxygen sensing and detection. This work provides a new idea to design pure organic discrete-molecule RTP materials with high efficiency, and TA derivatives show a potential to be applied in quantitative detection of oxygen as a new-generation optical oxygen-sensing material.

**Keywords:** pure organic room-temperature phosphorescence, discrete molecule, thianthrene, ratiometric optical oxygen sensing, polymer film, folding geometry, spin-orbit coupling

## 1 INTRODUCTION

Due to high efficiency and long lifetime of luminescence, phosphorescent materials have received increasing attention, resulting in their broad applications in light-emitting devices (Higginbotham et al., 2021; Wang J. et al., 2021; Zhang et al., 2021), information encryption and storage (Bian et al., 2018; Gu et al., 2018; She et al., 2021), biological imaging (Yang J. et al., 2018; Yang et al., 2021), photodynamic therapy (Shi et al., 2014; Wang et al., 2020), molecular detection and sensing (Yu et al., 2017; Zhou et al., 2019; Liu et al., 2020), etc. Most of the phosphorescent materials are focused on metal complexes [such as Os (Omar et al., 2018), Ir (Idris et al., 2021; Mao et al., 2021), and Pt (Yang X. et al., 2018; Stipurin and Strassner, 2021)], due to the strong spin-orbit coupling (SOC) from the heavy-atom effect of metal atoms. However, they still have some drawbacks from high cost, resource

scarcity, and potential toxicity of these noble metals, so the pure organic metal-free room-temperature phosphorescence (RTP) material becomes an ideal alternative. Limited by the weak SOC in pure organic materials, their phosphorescence radiation experiences an extremely slow process (Zhao et al., 2020), which leads to very easy deactivation of triplet excitons by molecular thermal motions or external oxygen quenching. In this case, two pathways are commonly used to obtain the efficient pure organic RTP: one is to promote the generation of triplet excitons by enhancing SOC effect with an introduction of heavy atoms (e.g., Br, I, and Se) (Wen et al., 2019; Lee et al., 2020) or heteroatoms (e.g., O, N, and S) (Xu et al., 2017; Wen et al., 2020; Xu et al., 2020; Wen et al., 2021) in molecular systems; the other one is to suppress the non-radiative decay of triplet excitons by strengthening the system rigidity from crystallization and host-guest interactions (Gu et al., 2019; Qu et al., 2019). However, this crystalline state greatly increases the difficulty of material processing and limits the practical applications of pure organic RTP materials. As a matter of fact, it is more convenient for organic emitters to be widely used in the form of amorphous film comparing with crystalline state, especially for the doped film with discrete molecules in polymer matrix, showing excellent processability. Nevertheless, the efficient discrete-molecule RTP materials in amorphous film have been rarely reported (Li et al., 2018; Ma et al., 2018; Ma et al., 2019; Zhang et al., 2020), because the discrete-molecule RTP in amorphous state frequently encounters a competitive non-radiative decay of triplet excitons. As for the reasons, on the one hand, the environmental rigidity is not large enough to effectively suppress the molecular vibrational quenching; on the other hand, triplet state oxygen can sensitively quench RTP through non-radiative energy transfer *via* molecular collisions under ambient conditions (Lee et al., 2013).

Using this unique oxygen-sensitive property, the pure organic RTP materials can be also applied in the optical oxygen sensing and detection, which involves many aspects of the application, such as physiological and pathological detection (Zhang et al., 2009; Spencer et al., 2014; Zhang et al., 2018), food packaging and storage (Smiddy et al., 2002; Mills, 2005; O'Mahony et al., 2006), and so on. Commonly, the ratiometric measurement method is used to improve the accuracy of optical oxygen detection, which combines an oxygen-insensitive fluorophore and an oxygen-sensitive phosphor into the same polymer matrix, and the oxygen concentration can be quantitatively detected by the ratio of emission intensities between fluorescence and phosphorescence (Feng et al., 2012). For the ratiometric measurement, the metal complex material with single phosphorescence usually needs to be used together with a fluorescence material (Xu et al., 2001), which easily leads to complex problems from multi-components, including sophisticated processing and physical separation (Huang et al., 2018). Thus, the pure organic discrete-molecule RTP material can be a good candidate for ratiometric measurement, because its moderate SOC enables simultaneous and comparable dual-emission between fluorescence and RTP. In addition, such a discrete-molecule dual-emission material is doped in polymer matrix, which surely facilitates the oxygen sensing and detection

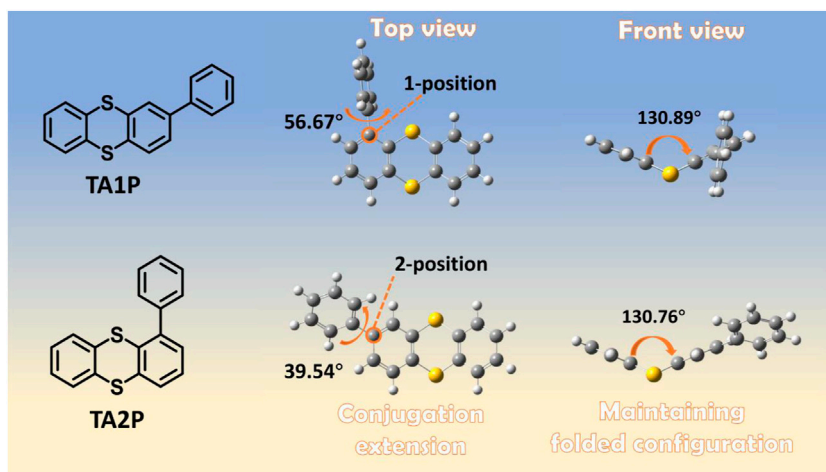
as a result of good oxygen permeability, unlike the difficult oxygen diffusion in tightly packed molecular crystals (Zhou et al., 2019).

In this work, we designed and synthesized two pure organic compounds, showing the efficient RTP of discrete molecule in polymer film for oxygen sensing and detection. Two compounds, 1-phenylthianthrene (TA1P) and 2-phenylthianthrene (TA2P), were obtained by a simple chemical modification of TA at 1- and 2-positions by using a single-phenyl group. When these two compounds were dispersed in polymethyl methacrylate (PMMA) matrix to form the discrete-molecule-doped film, they exhibit a strong RTP emission band after deoxygenation along with an almost constant fluorescence emission. The efficient RTP emission can be ascribed to the mechanism of folding-induced SOC enhancement (Liu et al., 2018). As a result, the fluorescence intensity can be directly used as a reference signal and RTP intensity can act as an analysis signal, which enable single-component ratiometric optical oxygen sensing and detection without any internal standard substance. Compared with TA1P, the  $\pi$ -conjugation of TA2P is enhanced due to the phenyl substitution at the 2-position of TA, resulting in a larger separation between fluorescence and RTP emission spectra, which substantially decreases the intensity interference between fluorescence and RTP. TA2P demonstrates a better linearity and a larger quenching constant than those of TA1P in oxygen-sensing experiment, which greatly improves the accuracy of oxygen sensing and detection. This work mainly presents a molecular design strategy of the efficient discrete-molecule RTP material, as well as their potential application in terms of oxygen sensing and detection.

## 2 MATERIALS AND METHODS

### 2.1 Materials and General Methods

All the reagents and solvents used for the synthesis were purchased commercially. The prepared compounds were characterized by  $^1\text{H}$  and  $^{13}\text{C}$  Nuclear magnetic resonance (NMR) spectra using tetramethylsilane (TMS) as the internal standard (Bruker AVANCE 500 spectrometer), mass spectra (Thermo Fisher ITQ1100 instrument), and elemental analysis (Flash EA 1112, CHNS elemental analysis instrument). UV-vis spectra of films were recorded on a Shimadzu UV-3100 Spectrophotometer. Emission spectra and time-resolved emission spectra were carried out on a FLS980 Spectrometer. Photoluminescence quantum yields under ambient conditions were measured by using an integrating sphere apparatus on a FLS980 Spectrometer, and the excitation wavelength was 300 nm. RTP efficiency was obtained by a comparison between fluorescence and RTP spectra areas under the same experimental conditions. Grayscale images and grayscale values were obtained by using a MATLAB program. The density functional theory (DFT) was adopted for the ground-state geometry optimization at the level of CAM-B3LYP/6-31G(d, p) using Gaussian 09 (version D.01) package (Frisch et al., 2013). The natural transition orbitals (NTOs) were calculated by using time-dependent DFT (TD-DFT) at the



**SCHEME 1** | Chemical structures and molecular geometries of TA1P and TA2P.

level of CAM-B3LYP/6-31G(d, p). SOC coefficients were quantitatively estimated at the level of CAM-B3LYP/6-31G(d, p) by using the Beijing Density Functional (BDF) program (Liu et al., 2003; Li et al., 2012; Quaranta et al., 2012; Li et al., 2013; Li et al., 2014).

## 2.2 Preparation of Film

Firstly, 1 mg TA derivative and 100 mg PMMA particles were weighed, and then both of them were put into a sample tube, followed by a solvent addition of 1.5 ml chloroform; the mixture was left for 30 min until the PMMA was completely dissolved; the mixture of TA derivative and PMMA was further well dispersed by sonicated treatment for 5 min to prepare a homogeneous stock solution. The stock solution was spin-coated on a quartz glass substrate, and a thin film for oxygen sensing and detection was successfully obtained after solvent evaporation and film drying in the air for 30 min.

## 2.3 Synthesis

### 2.3.1 The Synthesis of 1-Phenylthianthrene

A mixture of 1-thianthrenylboronic acid (520 mg, 2.00 mmol), bromobenzene (471 mg, 3.00 mmol),  $K_2CO_3$  (2.48 g, 18.00 mmol), 6 ml distilled water, and 9 ml toluene was degassed and recharged with nitrogen. Then,  $Pd(PPh_3)_4$  (69 mg, 0.06 mmol) was added in the mixture as catalyst, and the mixture was degassed and recharged with nitrogen again. After being stirred and refluxed at 90°C for 48 h under nitrogen atmosphere, the mixture was extracted with dichloromethane (DCM). The organic phase was dried with anhydrous sodium sulfate, filtered, and concentrated in vacuum. It was purified *via* silica gel chromatography by the mixture of petroleum ether/DCM and was recrystallized from DCM/methanol to give the product as white powder in 66% yield (385 mg).  $^1H$  NMR (500 MHz, DMSO- $d_6$ , 25°C, TMS):  $\delta$ =7.62 (ddd,  $J$  = 16.5, 7.7, and 1.4 Hz, 2H), 7.53 (dd,  $J$  = 8.0 and 6.5 Hz, 2H), 7.50–7.44 (m, 1H), 7.48–7.39 (m, 4H), 7.39–7.32 (m, 2H), and 7.28 (td,  $J$  = 7.5 and 1.4 Hz, 1H);  $^{13}C$  NMR (126 MHz,  $CDCl_3$ - $d$ , 25°C, TMS):  $\delta$  =

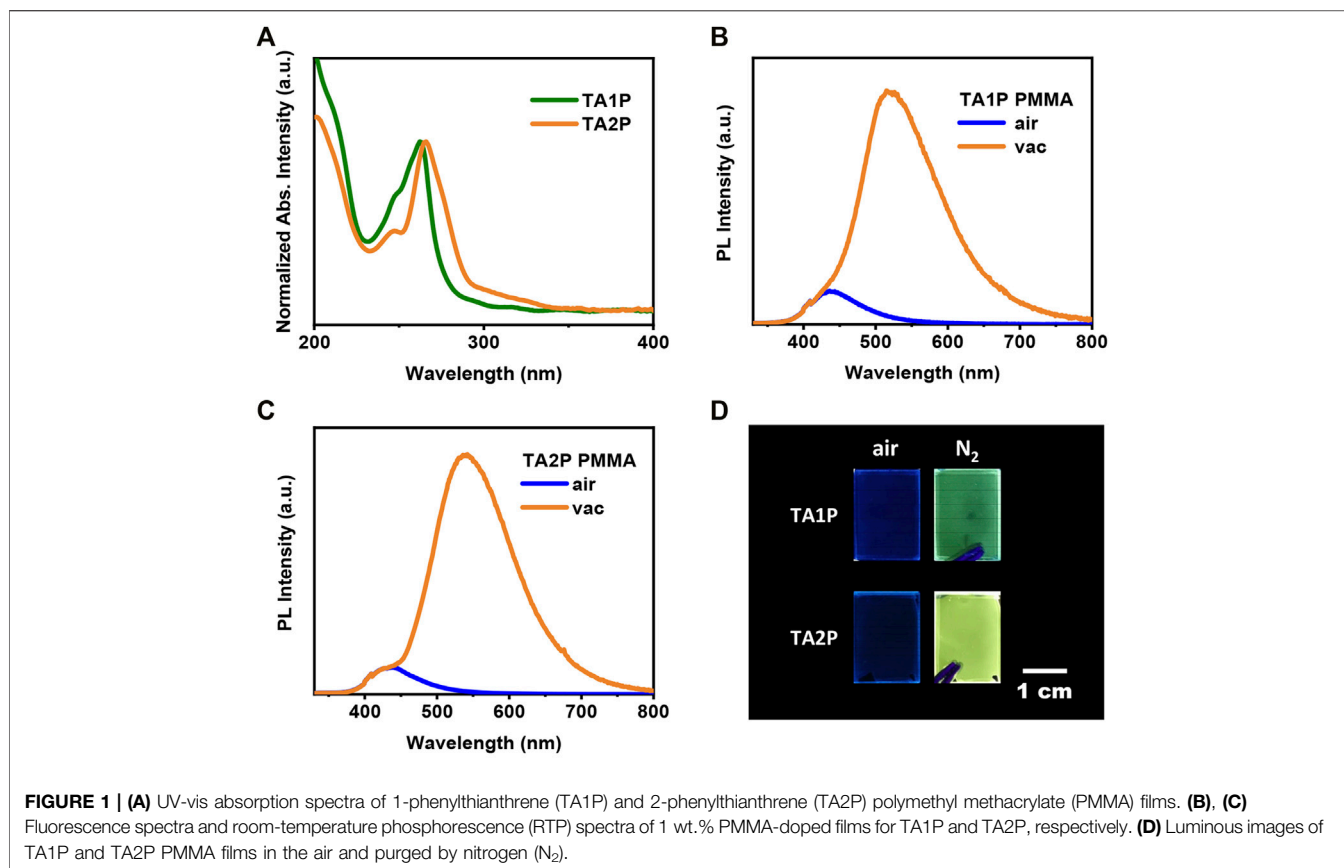
142.52 (C), 140.21 (C), 136.35 (C), 135.98 (C), 135.40 (C), 135.05 (C), 129.44 (CH), 129.28 (CH), 128.88 (CH), 128.52 (CH), 128.22 (CH), 128.15 (CH), 127.83 (CH), 127.77 (CH), 127.54 (CH), and 127.06 (CH). GC-MS, EI, mass  $m/z$ : 292.42 [ $M^+$ ]; anal. calculated for  $C_{12}H_{18}S_2$ : C 73.94, H 4.14, and S 21.93; found: C 73.97, H 4.20, and S 21.61.

### 2.3.2 The Synthesis of 2-Phenylthianthrene

According to a previous report, 2-bromothianthrene was synthesized (Liu et al., 2016). TA2P was synthesized by a procedure similar to that of TA1P, and the detail is shown in the **Supplementary Material**. TA2P product was obtained as white powder in 72% yield (420 mg).  $^1H$  NMR (500 MHz, DMSO- $d_6$ , 25°C, TMS):  $\delta$  = 7.87 (d,  $J$  = 1.3 Hz, 1H), 7.74–7.69 (m, 2H), 7.66 (d,  $J$  = 1.2 Hz, 2H), 7.61 (ddd,  $J$  = 5.5, 3.3, and 1.7 Hz, 2H), 7.48 (t,  $J$  = 7.6 Hz, 2H), and 7.39 (ddd,  $J$  = 13.1, 6.6, and 2.3 Hz, 3H);  $^{13}C$  NMR (126 MHz,  $CDCl_3$ - $d$ , 25°C, TMS):  $\delta$  = 141.09 (C), 139.69 (C), 136.14 (C), 135.57 (C), 135.46 (C), 134.39 (C), 128.91 (CH), 128.81 (CH), 128.76 (CH), 127.75 (CH), 127.28 (CH), 127.00 (CH), and 126.51 (CH). GC-MS, EI, mass  $m/z$ : 292.42 [ $M^+$ ]; anal. calculated for  $C_{12}H_{18}S_2$ : C 73.94, H 4.14, and S 21.93; found: C 74.22, H 4.04, and S 21.02.

## 3 RESULTS AND DISCUSSION

In our previous work, efficient RTP of TA was reported with a novel mechanism of folding-induced SOC enhancement. TA exhibits not only bright RTP in the crystalline state but also discrete-molecule RTP emission in the doped film of PMMA after deoxygenation. However, under ambient conditions, the discrete-molecule RTP emission cannot be observed in its doped film (**Supplementary Figure S1**), owing to the complete quenching of triplet state of TA by molecular oxygen in the air. Such a high oxygen sensitivity of TA-doped film inspires us to explore a unique application of TA and its derivatives in oxygen sensing and detection. However, for TA emission, due to the inadequate

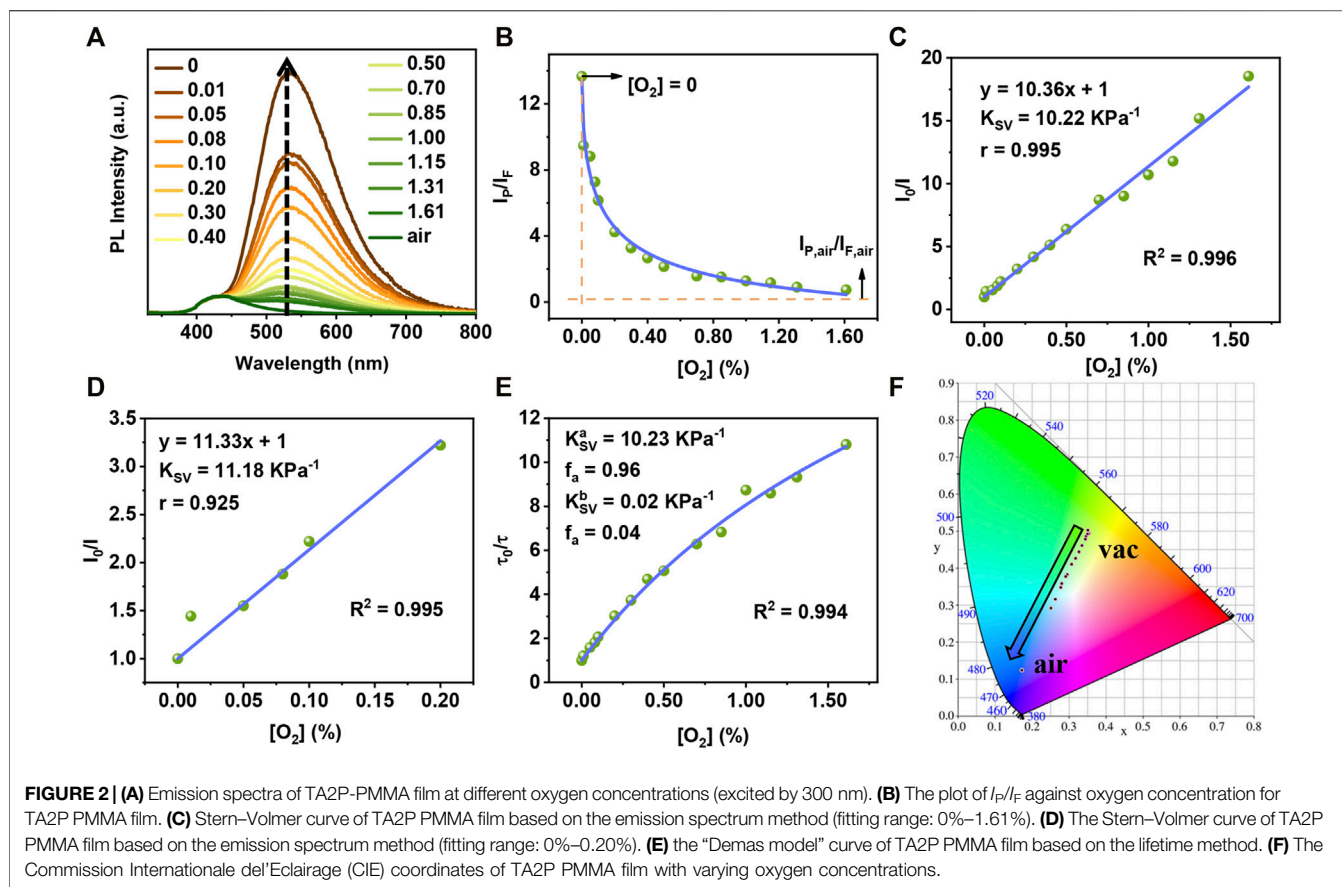


separation between fluorescence and RTP spectra, the fluorescence intensity is easily affected by the RTP intensity with the decrease of oxygen concentration, which will cause a serious error in ratiometric optical oxygen detection. How to achieve good separation between fluorescence and RTP spectra while maintaining high efficiency of discrete-molecule RTP is a primary focus for molecular design of oxygen-sensitive materials. As regards TA, its high-efficiency discrete-molecule RTP comes from the substantial SOC brought by the folded configuration. Therefore, we can obtain the impressive SOC by maintaining the folded configuration of TA and achieve good separation of fluorescence and RTP spectra by chemical modification of TA. For this reason, TA was further chemically modified at two main sites (1- and 2-position) to design two TA derivatives (TA1P and TA2P), respectively (**Scheme 1; Supplementary Scheme S1**).

For the oxygen sensing and detection, the polymer matrix is a key factor to determine its working performance. As a priority, PMMA was chosen as the polymer matrix for good film-forming ability, proper oxygen permeability, good UV transmittance, etc. (Wang and Wolfbeis, 2014) The experimental operation process is described in detail in the *Preparation of Film* section (**Supplementary Scheme S2**).

Compared with TA, both TA1P and TA2P exhibit different degrees of redshift in their absorption spectra, as a result of the different conjugation effect between phenyl group and TA unit (**Figure 1A; Supplementary Figures S2, S3**). Obviously, the substitution of phenyl at the 2-position of TA is more effective

for conjugation extension than that at the 1-position, and this difference can be clearly understood by theoretical calculations. In the ground state of TA1P (**Supplementary Figure S4**), the dihedral angle between phenyl group and TA unit is as large as  $56.67^\circ$  due to the steric hindrance. Although the phenyl group participates in the electronic transition of  $S_0 \rightarrow S_1$ , the degree of participation is very low, indicating a weak conjugation effect between the phenyl group and TA unit. However, for TA2P (**Supplementary Figure S5**), the small steric hindrance between phenyl group and TA unit results in a small dihedral angle of  $39.54^\circ$ , and the phenyl group obviously participates in the electronic transition of  $S_0 \rightarrow S_1$ , corresponding to an enhanced conjugation. As for emission, both compounds show almost the same blue emission under ambient conditions (the wavelength maximum is at 436 nm in PMMA-doped films). The time-resolved emission spectra demonstrate a short-lived characteristic, indicating the blue fluorescence for the discrete molecules in the doped films (**Supplementary Figures S6, S7**). As shown in **Figures 1B,C**, when the doped films are deoxygenated in a vacuum, both materials exhibit a new emission band (peaking at 519 and 533 nm for TA1P and TA2P, respectively) at the long wavelength in addition to the original weak fluorescence emission, and the new emission intensity far exceeds the fluorescence intensity in a vacuum. Time-resolved emission spectra reveal a long-lived characteristic of the long-wavelength emission bands (**Supplementary Figure S8**), corresponding to the RTP emission. Furthermore, when the



film was purged by using a nitrogen stream to simulate the deoxygenation environment, it is obvious that the emission color changes from faint blue to bright green or yellow for these two films (Figure 1D), in good agreement with the spectral measurement in the air and in a vacuum, respectively. Photoluminescence (PL) efficiency is an important performance parameter to evaluate RTP materials for ratiometric optical oxygen sensing and detection. Under ambient conditions, the PL efficiencies of TA1P and TA2P films are measured to be 0.89% and 1.73%, which correspond to their fluorescence efficiencies, respectively. Their RTP efficiencies are estimated to be 8.44% for TA1P and 22.73% for TA2P, which are very high values for pure organic discrete-molecule RTP materials. Compared with TA1P, TA2P has a much higher efficiency of RTP, which is surely more advantageous to be used for oxygen sensing and detection as a detection signal. To understand the origin of RTP of these two materials, the excited states and SOC coefficients were calculated between singlet and triplet states, respectively. Owing to the folding geometry of TA1P and TA2P (the folding dihedral angle is  $130.89^\circ$  and  $130.76^\circ$  for TA units in TA1P and TA2P, respectively), the SOC coefficients are estimated to be very sizeable between singlet and triplet manifolds, which are much higher than those of usual pure organic materials as a result of a new mechanism of folding-induced SOC enhancement. These large SOC coefficients provide very rich intersystem crossing (ISC) channels for the effective generation of triplet excitons, and

then the great SOC between  $T_1$  and  $S_0$  can ensure the efficient radiation of triplet excitons to produce efficient RTP emission (from Supplementary Figures S9–S12).

From qualitative sensing to quantitative detection of oxygen, the detection range should be taken into account firstly. For this reason, a series of nitrogen and oxygen mixtures were prepared with different oxygen concentrations. Considering the complete RTP quenching of discrete-molecule-doped film in the air, the mixed gas should be prepared with an oxygen concentration of less than 21% in later experiments. After careful optimization of conditions, the oxygen concentration range was selected from 0% to 1.61% for subsequent experiments of oxygen detection. For ratiometric oxygen detection, the stability of reference signal is an important factor that affects the accuracy of detection. As shown in Figures 1B,C, the fluorescence intensities of these two films are affected very little, even negligibly, when the RTP intensity is increased dramatically during deoxygenation. This property allows them to be used for single-component ratiometric optical oxygen detection, where the fluorescence emission can directly serve as the reference signal without the addition of an internal standard substance. With increasing oxygen concentration, the fluorescence intensities of the three films (TA, TA1P, and TA2P) were plotted together for the purpose of comparison (Supplementary Figure S13). Among them, the fluorescence intensity of TA2P has the smallest fluctuation with the change of oxygen concentration, demonstrating the best

stability of fluorescence intensity as the reference signal for ratiometric optical oxygen detection, which is ascribed to the largest spectral separation between fluorescence (peaking at 436 nm) and RTP (peaking at 533 nm) in essence.

Next, TA2P was taken as an example to carry out oxygen detection experiment. When exposed to the air, the RTP emission of TA2P-doped film is completely quenched, showing pure fluorescence emission. With the decrease of oxygen concentration, the RTP emission is enhanced gradually, while the fluorescence intensity remains almost the same during this process (**Figure 2A**). For ratiometric optical oxygen detection, a new variable  $I$  is defined as  $I_p/I_f$ , corresponding to a ratio of the RTP emission intensity ( $I_p$ ) to the fluorescence emission intensity ( $I_f$ ) at different oxygen concentrations. As shown in **Figure 2B**, an inverse proportional relation can be obtained for  $I$  as a function of oxygen concentration. With increasing oxygen concentration, the value of  $I$  gradually approaches to  $I_{p,air}/I_{f,air}$  where  $I_{p,air}$  and  $I_{f,air}$  represent the actual spectral intensity at 533 and 436 nm in the air, respectively. When the oxygen concentration is zero, the variable  $I$  is equal to  $I_0$  in a vacuum. In order to quantitatively evaluate oxygen sensitivity, a linear relationship can be well fitted between  $I_0/I$  and oxygen concentration according to the Stern–Volmer **Eq. 1** (Feng et al., 2012; Wang and Wolfbeis, 2014), as shown in **Figure 2C**:

$$\frac{I_0}{I} = \frac{\tau_0}{\tau} = 1 + K_{SV} [O_2] = 1 + k_q \tau_0 [O_2] \quad (1)$$

where  $K_{SV}$  is the Stern–Volmer quenching constant,  $k_q$  is quenching rate constant,  $[O_2]$  is the oxygen concentration, and  $\tau_0$  is the RTP lifetime when  $[O_2] = 0$ .

As a result, the linear fitting of TA2P-doped film shows excellent correlation in the  $[O_2]$  range of 0%–1.61%, and the correlation coefficient ( $R^2$ ) is as high as 0.996, corresponding to the Pearson correlation coefficient (Pearson's  $r$ ) of 0.995. The Stern–Volmer constant ( $K_{SV}$ ) is estimated to be  $10.22 \text{ KPa}^{-1}$ , which reflects very high oxygen sensitivity of TA2P film. When the linear fitting was done at an oxygen concentration lower than 0.2%, the correlation coefficient and  $K_{SV}$  are still as high as 0.994 and  $11.18 \text{ KPa}^{-1}$ , respectively (**Figure 2D**). This result can guarantee the accuracy of oxygen detection even at a very low oxygen concentration. In the meantime, to verify the dynamic quenching mechanism of oxygen detection, the RTP lifetimes of TA2P film were recorded at different oxygen concentrations. The Stern–Volmer curve of the  $\tau_0/\tau$  shows a slight curvature, which is common in most optical oxygen sensors due to the inevitable heterogeneity of materials. In fact, it can be rationalized that there are different micro-zones for the material in different micro-environments. And thus, the quenching constants may be different in different micro-environments, causing a linear deviation of the Stern–Volmer curve. In this case, it can be well described using the “two-site model” by Demas and co-workers, which is also called the “Demas model” **Eq. 2** (Carraway et al., 1991; Borisov et al., 2006; Medina-Castillo et al., 2007):

$$\frac{I_0}{I} = \frac{\tau_0}{\tau} = \frac{1}{\frac{f_a}{1+K_{SV}^a [O_2]} + \frac{f_b}{1+K_{SV}^b [O_2]}} \quad (2)$$

where,  $K_{SV}^a$  and  $K_{SV}^b$  are Stern–Volmer constants of different micro-zone components and  $f_a$  and  $f_b$  are their

corresponding component proportions ( $f_a + f_b = 1$ ), respectively.

As shown in **Figure 2E**, the Demas model is used for Stern–Volmer curve fitting, resulting in  $K_{SV}^a = 10.23 \text{ KPa}^{-1}$  with a large component ratio of 96% ( $f_a = 0.96$ ) as well as  $K_{SV}^b = 0.02 \text{ KPa}^{-1}$  with a small proportion of only 4% ( $f_b = 0.04$ ). Thus, the overall  $K_{SV}$  can be replaced with  $K_{SV}^a$  approximately, and  $K_{SV}^a$  is almost equal to the  $K_{SV}$  based on  $I_0/I$  from Stern–Volmer linear fitting according to **Eq. 1** (**Supplementary Figure S14**), which further validates a dynamic quenching mechanism of RTP in oxygen detection. Besides, the quenching rate constant ( $k_q$ ) can be calculated as  $213.8 \text{ KPa}^{-1} \text{ s}^{-1}$  by **Eq. 1**, which is one of the highest values among all oxygen-sensing materials (Zhou et al., 2019; Liu et al., 2020; Wang S. et al., 2021). For another key parameter for oxygen detection, the limit of detection (LOD) can be estimated as the oxygen concentration when  $I_p/I_f$  is changed by 0.1% (Guo et al., 2021). For TA2P-doped film, the LOD is calculated to be  $0.0979 \text{ Pa}$  (equal to 0.966 ppm at atmospheric pressure), which is among one of the best values for oxygen detection.

Owing to the significant difference between fluorescence and RTP spectra, the emission color change of TA2P can be observed with different oxygen concentrations. This color change can be expressed through the Commission Internationale de l'Éclairage (CIE) coordinates, as shown in **Figure 2F**. As the oxygen concentration gradually increases, the CIE coordinate points move along a line from yellow-green to blue region. Such a linear change gives us an inspiration to conduct the colorimetric detection of oxygen concentration, which is similar to the pH measurement using pH test strips. A simple home-made device was designed to detect the oxygen concentration of nitrogen–oxygen mixed gas stream (**Supplementary Figure S15**). As shown in **Figure 3**, when the TA2P film is purged by the mixture of nitrogen and oxygen with different oxygen contents, the color change can be obviously observed with the naked eye. At the same time, the luminous image can be transformed into a grayscale one, and the grayscale value is obtained with the help of computer software (Zhou et al., 2019). In the fitting range of 0.08%–1.15%, a good correlation linearity was found between grayscale value and oxygen concentration (**Supplementary Figure S16**), which provides a simple method for on-site detection of oxygen concentration in the absence of spectral measurement instrument.

Moreover, the PMMA polymer matrix was replaced with Zeonex<sup>®</sup> for optimizing oxygen detection (Tomkeviciene et al., 2019), in which Zeonex<sup>®</sup> is more oxygen-permeable and more rigid than PMMA. Due to the better oxygen permeability, the RTP of TA2P Zeonex<sup>®</sup> film can be greatly quenched at a lower oxygen concentration, (**Figure 4A**). Different from PMMA matrix, the Stern–Volmer curve obtained based on  $I_0/I$  with decreasing oxygen concentration shows an obvious non-linear change in the way of first flat and then steep, instead of a good linear fitting like that in PMMA matrix. Likewise, the Demas model was also used to fit the Stern–Volmer curve and to estimate  $K_{SV}$  (**Figure 4B**). As a result, its  $K_{SV}^a$  is calculated as high as  $111.86 \text{ KPa}^{-1}$  ( $f_a = 0.99$ , an almost complete contribution to  $K_{SV}$ ). Such a high  $K_{SV}$  is very rare in

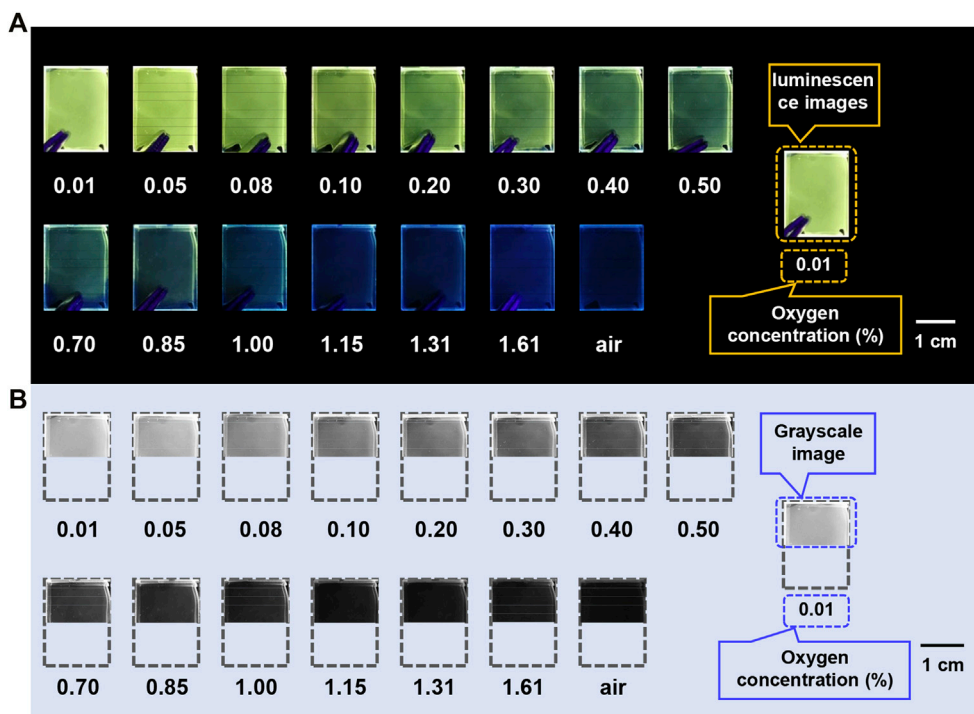


**FIGURE 3 | (A)** Luminescence images of TA2P PMMA-doped films at different oxygen concentrations. **(B)** Grayscale images corresponding to luminescence images at different oxygen concentrations.

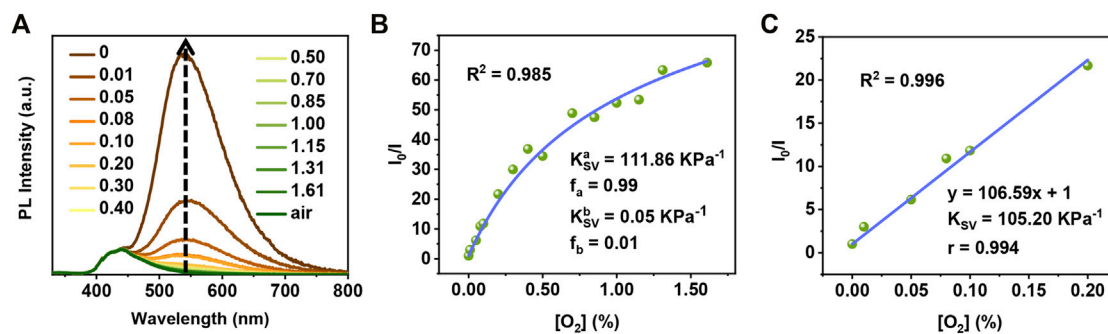


**FIGURE 4 | (A)** Emission spectra of TA2P Zeonex® film at different oxygen concentrations. **(B)** The Demas model curve of TA2P Zeonex® film (fitting range: 0%–1.61%). **(C)** The Stern–Volmer curve of TA2P Zeonex® film (fitting range: 0%–0.20%).

oxygen-sensing materials, and what is more, the Stern–Volmer curve still exhibits excellent linearity when the oxygen concentration is below 0.20% (**Figure 4C**). Also, the  $K_{SV}$  was obtained as  $104.62 \text{ KPa}^{-1}$  by direct linear fitting according to the Stern–Volmer Eq. 1, which is very close to the fitting result using the Demas model. Such a high sensitivity provides a feasible alternative to use TA2P Zeonex® film for an accurate detection of trace oxygen in the future (Borisov et al., 2011).

Relative to TA2P, TA1P shows an inferior performance in oxygen detection, and the detailed data is shown in **Supplementary Figures S17, S18**.

## 4 CONCLUSION

In summary, two phenyl-substituted derivatives of TA (TA1P and TA2P) were designed and synthesized for the efficient pure organic discrete-molecule RTP and the featured application of oxygen sensing and detection. These two compounds display the dual emission of fluorescence and RTP in discrete-molecule-doped film after deoxygenation, in which the efficient RTP is ascribed to the mechanism of folding-induced SOC enhancement. As a comparison, TA2P exhibits a higher RTP efficiency and more red-shifted RTP emission than those of TA1P, indicating a more significant electron conjugation effect

between TA and phenyl group. Thus, TA2P has merits of both high efficiency of RTP and large spectral separation between dual emissions, which is more suitable for discrete-molecule ratiometric optical oxygen sensing and detection. As a result, TA2P demonstrates a Stern–Volmer quenching constant as high as  $10.22 \text{ KPa}^{-1}$  and the LOD can reach as low as  $0.966 \text{ ppm}$  in PMMA-doped film, which is one of the best results among oxygen-sensing materials. Additionally, PMMA was replaced with Zeonex<sup>®</sup> as a polymer matrix for further performance optimization. The Stern–Volmer constant of TA2P is estimated to be  $111.86 \text{ KPa}^{-1}$  in Zeonex<sup>®</sup> matrix, which is a very high value. These results present a feasible way for the optimization design of pure organic discrete-molecule RTP materials based on TA derivatives, as well as provide a class of dual-emission materials for a promising application in ratiometric optical oxygen sensing and detection.

## DATA AVAILABILITY STATEMENT

The original contributions presented in the study are included in the article/**Supplementary Material**; further inquiries can be directed to the corresponding authors.

## REFERENCES

- Bian, L., Shi, H., Wang, X., Ling, K., Ma, H., Li, M., et al. (2018). Simultaneously Enhancing Efficiency and Lifetime of Ultralong Organic Phosphorescence Materials by Molecular Self-Assembly. *J. Am. Chem. Soc.* 140 (34), 10734–10739. doi:10.1021/jacs.8b03867
- Borisov, S. M., Lehner, P., and Klimant, I. (2011). Novel Optical Trace Oxygen Sensors Based on Platinum(II) and Palladium(II) Complexes with 5,10,15,20-Meso-Tetrakis-(2,3,4,5,6-Pentafluorophenyl)-Porphyrin Covalently Immobilized on Silica-Gel Particles. *Analytica Chim. Acta.* 690 (1), 108–115. doi:10.1016/j.aca.2011.01.057
- Borisov, S. M., Vasylevska, A. S., Krause, C., and Wolfbeis, O. S. (2006). Composite Luminescent Material for Dual Sensing of Oxygen and Temperature. *Adv. Funct. Mater.* 16 (12), 1536–1542. doi:10.1002/adfm.200500778
- Carraway, E. R., Demas, J. N., DeGraff, B. A., and Bacon, J. R. (1991). Photochemistry and Photochemistry of Oxygen Sensors Based on Luminescent Transition-Metal Complexes. *Anal. Chem.* 63 (4), 337–342. doi:10.1021/ac00004a007
- Feng, Y., Cheng, J., Zhou, L., Zhou, X., and Xiang, H. (2012). Ratiometric Optical Oxygen Sensing: a Review in Respect of Material Design. *Analyst.* 137 (21), 4885–4901. doi:10.1039/C2AN35907C
- Frisch, M. J., Trucks, G. W., Schlegel, H. B., Scuseria, G. E., Robb, M. A., Cheeseman, J. R., et al. (2013). *Gaussian 09, Revision D.01*. Wallingford CT: Gaussian, Inc.
- Gu, L., Shi, H., Bian, L., Gu, M., Ling, K., Wang, X., et al. (2019). Colour-Tunable Ultra-Long Organic Phosphorescence of a Single-Component Molecular crystal. *Nat. Photon.* 13 (6), 406–411. doi:10.1038/s41566-019-0408-4
- Gu, L., Shi, H., Gu, M., Ling, K., Ma, H., Cai, S., et al. (2018). Dynamic Ultralong Organic Phosphorescence by Photoactivation. *Angew. Chem. Int. Ed.* 57 (28), 8425–8431. doi:10.1002/anie.201712381
- Guo, W.-J., Chen, Y.-Z., Tung, C.-H., and Wu, L.-Z. (2021). Ultralong Room-Temperature Phosphorescence of Silicon-Based Pure Organic Crystal for Oxygen Sensing. *CCS Chem.* 3, 1384–1392. doi:10.31635/ccschem.021.202100932
- Higginbotham, H. F., Okazaki, M., de Silva, P., Minakata, S., Takeda, Y., and Data, P. (2021). Heavy-Atom-Free Room-Temperature Phosphorescent Organic

## AUTHOR CONTRIBUTIONS

ZY and HL provided the molecular design and performed the synthesis experiment. ZY, SZ, XZ, and ML carried out the photophysical characterizations and image collection. ZY carried out the theoretical calculations. HL and BY supervised the whole work. All authors contributed to the article and approved the submitted version.

## FUNDING

This work was supported by the National Natural Science Foundation of China (51873077, 91833304, 52073117, and 52103209), the National Key Research and Development Program of China (2020YFA0714603), and the China Postdoctoral Science Foundation (2018M641767).

## SUPPLEMENTARY MATERIAL

The Supplementary Material for this article can be found online at: <https://www.frontiersin.org/articles/10.3389/fchem.2021.810304/full#supplementary-material>

- Light-Emitting Diodes Enabled by Excited States Engineering. *ACS Appl. Mater. Inter.* 13 (2), 2899–2907. doi:10.1021/acsami.0c17295
- Huang, X., Song, J., Yung, B. C., Huang, X., Xiong, Y., and Chen, X. (2018). Ratiometric Optical Nanoprobes Enable Accurate Molecular Detection and Imaging. *Chem. Soc. Rev.* 47 (8), 2873–2920. doi:10.1039/C7CS00612H
- Idris, M., Kapper, S. C., Tadle, A. C., Batagoda, T., Muthiah Ravinson, D. S., Abimbola, O., et al. (2021). Blue Emissive Fac/Mer-Iridium (III) NHC Carbene Complexes and Their Application in OLEDs. *Adv. Opt. Mater.* 9 (8), 2001994. doi:10.1002/adom.202001994
- Lee, D., Bolton, O., Kim, B. C., Youk, J. H., Takayama, S., and Kim, J. (2013). Room Temperature Phosphorescence of Metal-Free Organic Materials in Amorphous Polymer Matrices. *J. Am. Chem. Soc.* 135 (16), 6325–6329. doi:10.1021/ja401769g
- Lee, D. R., Lee, K. H., Shao, W., Kim, C. L., Kim, J., and Lee, J. Y. (2020). Heavy Atom Effect of Selenium for Metal-Free Phosphorescent Light-Emitting Diodes. *Chem. Mater.* 32 (6), 2583–2592. doi:10.1021/acs.chemmater.0c00078
- Li, D., Lu, F., Wang, J., Hu, W., Cao, X.-M., Ma, X., et al. (2018). Amorphous Metal-Free Room-Temperature Phosphorescent Small Molecules with Multicolor Photoluminescence via a Host-Guest and Dual-Emission Strategy. *J. Am. Chem. Soc.* 140 (5), 1916–1923. doi:10.1021/jacs.7b12800
- Li, Z., Suo, B., Zhang, Y., Xiao, Y., and Liu, W. (2013). Combining Spin-Adapted Open-Shell TD-DFT with Spin-Orbit Coupling. *Mol. Phys.* 111 (24), 3741–3755. doi:10.1080/00268976.2013.785611
- Li, Z., Xiao, Y., and Liu, W. (2012). On the Spin Separation of Algebraic Two-Component Relativistic Hamiltonians. *J. Chem. Phys.* 137 (15), 154114. doi:10.1063/1.4758987
- Li, Z., Xiao, Y., and Liu, W. (2014). On the Spin Separation of Algebraic Two-Component Relativistic Hamiltonians: Molecular Properties. *J. Chem. Phys.* 141 (5), 054111. doi:10.1063/1.4891567
- Liu, H., Gao, Y., Cao, J., Li, T., Wen, Y., Ge, Y., et al. (2018). Efficient Room-Temperature Phosphorescence Based on a Pure Organic Sulfur-Containing Heterocycle: Folding-Induced Spin-Orbit Coupling Enhancement. *Mater. Chem. Front.* 2 (10), 1853–1858. doi:10.1039/c8qm00320c
- Liu, H., Yao, L., Li, B., Chen, X., Gao, Y., Zhang, S., et al. (2016). Excimer-Induced High-Efficiency Fluorescence Due to Pairwise Anthracene Stacking in a Crystal with Long Lifetime. *Chem. Commun.* 52 (46), 7356–7359. doi:10.1039/C6CC01993E

- Liu, W., Wang, F., and Li, L. (2003). The Beijing Density Functional (BDF) Program Package: Methodologies and Applications. *J. Theor. Comput. Chem.* 02 (02), 257–272. doi:10.1142/s0219633603000471
- Liu, X. Q., Zhang, K., Gao, J. F., Chen, Y. Z., Tung, C. H., and Wu, L. Z. (2020). Monochromophore-Based Phosphorescence and Fluorescence from Pure Organic Assemblies for Ratiometric Hypoxia Detection. *Angew. Chem. Int. Ed.* 59 (52), 23456–23460. doi:10.1002/anie.202007039
- Ma, X., Wang, J., and Tian, H. (2019). Assembling-Induced Emission: An Efficient Approach for Amorphous Metal-Free Organic Emitting Materials with Room-Temperature Phosphorescence. *Acc. Chem. Res.* 52 (3), 738–748. doi:10.1021/acs.accounts.8b00620
- Ma, X., Xu, C., Wang, J., and Tian, H. (2018). Amorphous Pure Organic Polymers for Heavy-Atom-Free Efficient Room-Temperature Phosphorescence Emission. *Angew. Chem. Int. Ed.* 57 (34), 10854–10858. doi:10.1002/anie.201803947
- Mao, M.-X., Li, F.-L., Shen, Y., Liu, Q.-M., Xing, S., Luo, X.-F., et al. (2021). Simple Synthesis of Red Iridium(III) Complexes with Sulfur-Contained Four-Membered Ancillary Ligands for OLEDs. *Molecules.* 26 (9), 2599. doi:10.3390/molecules26092599
- Medina-Castillo, A. L., Fernández-Sánchez, J. F., Klein, C., Nazeeruddin, M. K., Segura-Carretero, A., Fernández-Gutiérrez, A., et al. (2007). Engineering of Efficient Phosphorescent Iridium Cationic Complex for Developing Oxygen-Sensitive Polymeric and Nanostructured Films. *Analyst.* 132 (9), 929–936. doi:10.1039/B702628E
- Mills, A. (2005). Oxygen Indicators and Intelligent Inks for Packaging Food. *Chem. Soc. Rev.* 34 (12), 1003–1011. doi:10.1039/B503997P
- O'Mahony, F. C., O'Riordan, T. C., Papkovskaia, N., Kerry, J. P., and Papkovsky, D. B. (2006). Non-Destructive Assessment of Oxygen Levels in Industrial Modified Atmosphere Packaged Cheddar Cheese. *Food Control.* 17 (4), 286–292. doi:10.1016/j.foodcont.2004.10.013
- Omar, S. A. E., Scattergood, P. A., McKenzie, L. K., Jones, C., Patmore, N. J., Meijer, A. J. H. M., et al. (2018). Photophysical and Cellular Imaging Studies of Brightly Luminescent Osmium(II) Pyridyltriazole Complexes. *Inorg. Chem.* 57 (21), 13201–13212. doi:10.1021/acs.inorgchem.8b01627
- Qu, G., Zhang, Y., and Ma, X. (2019). Recent Progress on Pure Organic Room Temperature Phosphorescence Materials Based on Host-Guest Interactions. *Chin. Chem. Lett.* 30 (10), 1809–1814. doi:10.1016/j.ccllet.2019.07.042
- Quaranta, M., Borisov, S. M., and Klimant, I. (2012). Indicators for Optical Oxygen Sensors. *Bioanal. Rev.* 4 (2-4), 115–157. doi:10.1007/s12566-012-0032-y
- She, P., Qin, Y., Ma, Y., Li, F., Lu, J., Dai, P., et al. (2021). Lifetime-Tunable Organic Persistent Room-Temperature Phosphorescent Salts for Large-Area Security Printing. *Sci. China Mater.* 64 (6), 1485–1494. doi:10.1007/s40843-020-1544-6
- Shi, H., Ma, X., Zhao, Q., Liu, B., Qu, Q., An, Z., et al. (2014). Ultrasmall Phosphorescent Polymer Dots for Ratiometric Oxygen Sensing and Photodynamic Cancer Therapy. *Adv. Funct. Mater.* 24 (30), 4823–4830. doi:10.1002/adfm.201400647
- Smiddy, M., Papkovskaia, N., Papkovsky, D. B., and Kerry, J. P. (2002). Use of Oxygen Sensors for the Non-Destructive Measurement of the Oxygen Content in Modified Atmosphere and Vacuum Packs of Cooked Chicken Patties; Impact of Oxygen Content on Lipid Oxidation. *Food Res. Int.* 35 (6), 577–584. doi:10.1016/S0963-9969(01)00160-0
- Spencer, J. A., Ferraro, F., Roussakis, E., Klein, A., Wu, J., Runnels, J. M., et al. (2014). Direct Measurement of Local Oxygen Concentration in the Bone Marrow of Live Animals. *Nature.* 508 (7495), 269–273. doi:10.1038/nature13034
- Stipurin, S., and Strassner, T. (2021). Phosphorescent Cyclometalated Platinum(II) Imidazolynylidene Complexes. *Eur. J. Inorg. Chem.* 2021 (9), 804–813. doi:10.1002/ejic.202001077
- Tomkeviciene, A., Dabulienė, A., Matulaitis, T., Guzauskas, M., Andruleviciene, V., Grazulevicius, J. V., et al. (2019). Bipolar Thianthrene Derivatives Exhibiting Room Temperature Phosphorescence for Oxygen Sensing. *Dyes Pigm.* 170, 107605. doi:10.1016/j.dyepig.2019.107605
- Wang, J., Liang, B., Wei, J., Li, Z., Xu, Y., Yang, T., et al. (2021). Highly Efficient Electrofluorescence Material Based on Pure Organic Phosphor Sensitization. *Angew. Chem. Int. Ed.* 60 (28), 15335–15339. doi:10.1002/anie.202104755
- Wang, S., Shu, H., Han, X., Wu, X., Tong, H., and Wang, L. (2021). A Highly Efficient Purely Organic Room-Temperature Phosphorescence Film Based on a Selenium-Containing Emitter for Sensitive Oxygen Detection. *J. Mater. Chem. C.* 9 (31), 9907–9913. doi:10.1039/D1TC02324A
- Wang, S., Xu, M., Huang, K., Zhi, J., Sun, C., Wang, K., et al. (2020). Biocompatible Metal-Free Organic Phosphorescent Nanoparticles for Efficiently Multidrug-Resistant Bacteria Eradication. *Sci. China Mater.* 63 (2), 316–324. doi:10.1007/s40843-019-1191-9
- Wang, X.-d., and Wolfbeis, O. S. (2014). Optical Methods for Sensing and Imaging Oxygen: Materials, Spectroscopies and Applications. *Chem. Soc. Rev.* 43 (10), 3666–3761. doi:10.1039/C4CS00039K
- Wen, Y., Liu, H., Zhang, S.-T., Pan, G., Yang, Z., Lu, T., et al. (2021). Modulating Room Temperature Phosphorescence by Oxidation of Thianthrene to Achieve Pure Organic Single-Molecule White-Light Emission. *CCS Chem.* 3 (7), 1940–1948. doi:10.31635/ccschem.020.202000433
- Wen, Y., Liu, H., Zhang, S., Cao, J., De, J., and Yang, B. (2020). Achieving Highly Efficient Pure Organic Single-Molecule White-Light Emitter: The Coenhanced Fluorescence and Phosphorescence Dual Emission by Tailoring Alkoxy Substituents. *Adv. Opt. Mater.* 8 (7), 1901995. doi:10.1002/adom.201901995
- Wen, Y., Liu, H., Zhang, S., Gao, Y., Yan, Y., and Yang, B. (2019). One-dimensional  $\pi$ - $\pi$  Stacking Induces Highly Efficient Pure Organic Room-Temperature Phosphorescence and Ternary-Emission Single-Molecule White Light. *J. Mater. Chem. C.* 7 (40), 12502–12508. doi:10.1039/c9tc04580e
- Xu, B., Wu, H., Chen, J., Yang, Z., Yang, Z., Wu, Y.-C., et al. (2017). White-light Emission from a Single Heavy Atom-free Molecule with Room Temperature Phosphorescence, Mechanochromism and Thermochromism. *Chem. Sci.* 8 (3), 1909–1914. doi:10.1039/C6SC03038F
- Xu, H., Aylott, J. W., Kopelman, R., Miller, T. J., and Philbert, M. A. (2001). A Real-Time Ratiometric Method for the Determination of Molecular Oxygen inside Living Cells Using Sol-Gel-Based Spherical Optical Nanosensors with Applications to Rat C6 Glioma. *Anal. Chem.* 73 (17), 4124–4133. doi:10.1021/ac102718
- Xu, L., Zhou, K., Qiu, X., Rao, B., Pei, D., Li, A., et al. (2020). Tunable Ultralong Organic Phosphorescence Modulated by Main-Group Elements with Different Lewis Acidity and Basicity. *J. Mater. Chem. C* 8 (42), 14740–14747. doi:10.1039/d0tc02953j
- Yang, J., Zhang, Y., Wu, X., Dai, W., Chen, D., Shi, J., et al. (2021). Rational Design of Pyrrole Derivatives with Aggregation-Induced Phosphorescence Characteristics for Time-Resolved and Two-Photon Luminescence Imaging. *Nat. Commun.* 12 (1). doi:10.1038/s41467-021-25174-6
- Yang, J. J., Zhen, X., Wang, B., Gao, X., Ren, Z., Wang, J., et al. (2018). The Influence of the Molecular Packing on the Room Temperature Phosphorescence of Purely Organic Luminogens. *Nat. Commun.* 9 (1), 1–10. doi:10.1038/s41467-018-03236-6
- Yang, X., Jiao, B., Dang, J.-S., Sun, Y., Wu, Y., Zhou, G., et al. (2018). Achieving High-Performance Solution-Processed Orange OLEDs with the Phosphorescent Cyclometalated Trinuclear Pt(II) Complex. *ACS Appl. Mater. Inter.* 10 (12), 10227–10235. doi:10.1021/acsami.7b18330
- Yu, Y., Kwon, M. S., Jung, J., Zeng, Y., Kim, M., Chung, K., et al. (2017). Room-Temperature-Phosphorescence-Based Dissolved Oxygen Detection by Core-Shell Polymer Nanoparticles Containing Metal-Free Organic Phosphors. *Angew. Chem. Int. Ed.* 56 (51), 16207–16211. doi:10.1002/anie.201708606
- Zhang, G., Palmer, G. M., Dewhirst, M. W., and Fraser, C. L. (2009). A Dual-Emissive-Materials Design Concept Enables Tumour Hypoxia Imaging. *Nat. Mater.* 8 (9), 747–751. doi:10.1038/nmat2509
- Zhang, K. Y., Yu, Q., Wei, H., Liu, S., Zhao, Q., and Huang, W. (2018). Long-Lived Emissive Probes for Time-Resolved Photoluminescence Bioimaging and Biosensing. *Chem. Rev.* 118 (4), 1770–1839. doi:10.1021/acs.chemrev.7b00425
- Zhang, T., Ma, X., Wu, H., Zhu, L., Zhao, Y., and Tian, H. (2020). Molecular Engineering for Metal-Free Amorphous Materials with Room-Temperature Phosphorescence. *Angew. Chem. Int. Ed.* 59 (28), 11206–11216. doi:10.1002/anie.201915433
- Zhang, Y., Su, Y., Wu, H., Wang, Z., Wang, C., Zheng, Y., et al. (2021). Large-Area, Flexible, Transparent, and Long-Lived Polymer-Based Phosphorescence Films. *J. Am. Chem. Soc.* 143 (34), 13675–13685. doi:10.1021/jacs.1c05213

Zhao, W., He, Z., and Tang, B. Z. (2020). Room-temperature Phosphorescence from Organic Aggregates. *Nat. Rev. Mater.* 5 (12), 869–885. doi:10.1038/s41578-020-0223-z

Zhou, Y., Qin, W., Du, C., Gao, H., Zhu, F., and Liang, G. (2019). Long-Lived Room-Temperature Phosphorescence for Visual and Quantitative Detection of Oxygen. *Angew. Chem. Int. Ed.* 58 (35), 12102–12106. doi:10.1002/anie.201906312

**Conflict of Interest:** The authors declare that the research was conducted in the absence of any commercial or financial relationships that could be construed as a potential conflict of interest.

The handling Editor declared a past co-authorship with one of the authors BY.

**Publisher's Note:** All claims expressed in this article are solely those of the authors and do not necessarily represent those of their affiliated organizations, or those of the publisher, the editors and the reviewers. Any product that may be evaluated in this article, or claim that may be made by its manufacturer, is not guaranteed or endorsed by the publisher.

*Copyright © 2022 Yang, Zhao, Zhang, Liu, Liu and Yang. This is an open-access article distributed under the terms of the Creative Commons Attribution License (CC BY). The use, distribution or reproduction in other forums is permitted, provided the original author(s) and the copyright owner(s) are credited and that the original publication in this journal is cited, in accordance with accepted academic practice. No use, distribution or reproduction is permitted which does not comply with these terms.*